The physical boundaries of public goods cooperation between surface-attached bacterial cells

Michael Weigert[1, 2, *] and Rolf Kümmerli[1, *]

* Corresponding authors

[1] Department of Plant- and Microbial Biology, University of Zurich, Winterthurerstrasse 190, 8057 Zurich, Switzerland

[2] Microbiology, Department of Biology I, Ludwig Maximilians University Munich, Grosshaderner Strasse 2-4, Martinsried, 82152, Germany.

* Correspondence address: Department of Plant- and Microbial Biology, University of Zurich, Winterthurerstrasse 190, 8057 Zurich, Switzerland. Tel: +41 44 635 2907; Fax: +41 44 635 2920; E-mail: rolf.kuemmerli@uzh.ch, michael_weigert@gmx.net

Abstract

Bacteria secrete a variety of compounds important for nutrient scavenging, competition mediation and infection establishment. While there is a general consensus that secreted compounds can be shared and therefore have social consequences for the bacterial collective, we know little about the physical limits of such bacterial social interactions. Here, we address this issue by studying the sharing of iron-scavenging siderophores between surface-attached microcolonies of the bacterium *Pseudomonas aeruginosa*. Using single-cell fluorescent microscopy, we show that siderophores, secreted by producers, quickly reach non-producers within a range of 100 µm, and significantly boost their fitness. Producers in turn respond to variation in sharing efficiency by adjusting their pyoverdine investment levels. These social effects wane with larger cell-to-cell distances and on hard surfaces. Thus, our findings reveal the boundaries of compound sharing, and show that sharing is particularly relevant between nearby yet physically separated bacteria on soft surfaces, matching realistic natural conditions.

Introduction

The study of cooperative interactions in bacteria is of interdisciplinary interest, as it is relevant for understanding microbial community assembly (Leinweber et al. 2017; Jousset et al. 2013), the establishment of infections (Köhler et al. 2009; Alizon and Lion 2011; Pollitt et al. 2014) , and biotechnological processes (Bachmann et al. 2016). Bacteria exhibit a wide range of cooperative traits, including the formation of biofilms and fruiting bodies, the secretion of toxins to infect hosts, coordinated swarming, and the scavenging of nutrients from the environment through the secretion of shareable compounds, such as enzymes and siderophores (West, Diggle, et al. 2007; Nadell et al. 2009). While the existing body of work has greatly changed our perception of bacteria – from simple autarkic individuals to sophisticated organisms, interacting and cooperating with each other – there are still considerable knowledge gaps. For instance, many of the insights gained on the sharing of public goods are based on experiments in planktonic batch cultures, where behavioural responses are averaged across millions of cells. This contrasts with the natural lifestyle of bacteria, where individual cells adhere to surfaces and form biofilms, and primarily interact with their immediate neighbours at the micrometre scale (Nadell and Bassler 2011; Drescher et al. 2014). The mismatch between laboratory and natural conditions has led to controversies in the field regarding the general relevance of microbial cooperation (Foster and Bell 2012; Zhang and Rainey 2013; Julou et al. 2013).

In our paper, we tackle these issues by testing whether and to what extent, secreted siderophores are shared between surface-attached individuals of the bacterium *Pseudomonas aeruginosa* using fluorescent microscopy. Siderophores are secondary metabolites produced by bacteria to scavenge iron from the environment, where it typically occurs in its insoluble ferric form or is actively withhold by the host in the context of infections (Ratledge and Dover 2000; Miethke

and Marahiel 2007). In our experiments, we examined the production and secretion of pyoverdine, the main siderophore of *P. aeruginosa* (Visca et al. 2007), which has become a model trait to study cooperation in bacteria, because it fulfils all the criteria of a cooperative trait: it is costly to produce and secreted outside the cell, where it generates benefits in iron-limited media for the producer itself, but also for nearby individuals with a compatible receptor for uptake (Griffin et al. 2004; Buckling et al. 2007; Inglis et al. 2016). Although highly influential, many of the insights gained, are based on batch culture experiments, which tell us little about whether pyoverdine is also shared in surface-attached communities, where molecule diffusion might be limited, and thus the range of sharing constrained (Kümmerli, Gardner, et al. 2009; Julou et al. 2013). However, such knowledge is key to understand whether public goods cooperation occurs in natural settings and in infections, where bacteria typically live in biofilms attached to organic and inorganic substrates (Nadell et al. 2009; Flemming et al. 2016).

Here, we present data from fluorescence time-laps microscopy experiments that examined bacterial interactions in real time at the micrometer scale. First, we tested whether pyoverdine molecules, secreted by producing cells, reach individuals that cannot produce pyoverdine themselves but have the receptor for uptake. Such evidence would be a direct demonstration of cooperation. We addressed this question by making use of the auto-fluorescent properties of pyoverdine, which enables us to quantify the amount of pyoverdine that is actually taken up by non-producer cells. Second, we hypothesis that if pyoverdine is shared then it can serve as a signalling molecule (Lamont et al. 2002), and producers should thus respond to changes in their social neighbourhood. Specifically, we predict that lower pyoverdine investment is required in a cooperative neighbourhood due to the efficient reciprocal pyoverdine sharing between cells, whereas non-producers act as a sink for pyoverdine and should therefore trigger increased investment levels to compensate for the loss of pyoverdine (Kümmerli, Jiricny, et al. 2009; F

Harrison 2013b). To test this hypothesis, we used a strain with a fluorescent gene reporter fusion to follow plastic responses in pyoverdine investment over time. Third, we examined whether pyoverdine diffusivity limits the range across which pyoverdine can be efficiently shared. To this end, we manipulated both the media viscosity, which directly affects molecule diffusion, and the distance between producer and non-producer cells, which increases the diffusion time and possibly reduces the amount of pyoverdine reaching non-producers. Finally, we used time-laps microscopy to quantify fitness effects of pyoverdine production and sharing in growing micro-colonies. Taken together, our experiments shed light on the physical boundaries and individual fitness consequences of public goods sharing.

Results

Pyoverdine diffuses from producers to non-producers

We put mono- and mixed cultures of the wildtype strain PAO1 (featuring a *pvdA*-gfp reporter fusion; see below) and its isogenic mutant PAO1*ΔpvdD* (tagged with a fitness-neutral mCherry marker, Figure S1), deficient for pyoverdine production, on small iron-limited agarose pads on a sealed microscopy slide (see Material and Methods for details). Cultures were highly diluted such that single cells were physically separated from each another at the beginning of the experiment. We then monitored the pyoverdine fluorescence in growing micro-colonies over time for both strains under the microscope. Pyoverdine fluorescence is predominantly visible in the periplasma, where molecule maturation occurs and when it is not bound to iron (Julou et al. 2013; Schalk and Guillon 2013). We found that fluorescence in non-producer colonies was indistinguishable from background signal one hour after incubation, indicating that no detectable pyoverdine had yet been taken up (Figure 1A+C). However, pyoverdine fluorescence signal in non-producer cells significantly increased above background level in mixed cultures after three hours (LM: $F_{5,7567} = 913$, $p < 0.001$) and peaked after five hours (t-

test: $t_{3945} = 79.33$, $p < 0.001$, Figure 1A+D). This demonstrates that significant amounts of pyoverdine diffuse from producer to non-producer microcolonies even when there is no direct cell-to-cell contact.

Producers adjust pyoverdine investment in the presence of non-producers

To test whether producers respond to changes in their social environment, we followed the expression pattern of *pvdA* (a gene involved in pyoverdine synthesis) and natural pyoverdine fluorescence in growing producer microcolonies over time (Figure 2). In our control treatment with added iron, both *pvdA* and pyoverdine signal were significantly downregulated compared to iron-limited conditions, demonstrating the functioning and high sensitivity of our reporters. Under iron limitation, meanwhile, *pvdA*-expression was significantly higher in mixed compared to monoculture at one hour (t-test: $t_{115} = 5.23$, $p < 0.001$) and three hours ($t_{860} = 13.92$, $p < 0.001$) post-incubation (Figure 2A). Pyoverdine fluorescence mirrored *pvdA* expression patterns, with higher pyoverdine levels being detected in producer cells growing in mixed cultures (Figure 2B), although the difference was only significant after three hours (t-test: $t_{992} = 13.30$, $p < 0.001$), and not after one hour (t-test: $t_{88} = 1.26$, $p = 0.211$). The picture changed five hours post-incubation, where both *pvdA*-expression and pyoverdine fluorescence were significantly lower in mixed compared to monocultures (for pvdA-expression: $t_{6441} = -16.67$, $p < 0.001$, for pyoverdine fluorescence: $t_{6017} = -50.01$, $p < 0.001$). These analyses demonstrate that producers rapidly alter pyovedine investment in response to the presence of non-producers, a pattern that can only be explained when pyoverdine is shared and is used as signal to perceive changes in the social environment.

Pyoverdine non-producers outgrow producers in mixed cultures

After having established that pyoverdine is shared between neighbouring, but physically separated surface-attached microcolonies, we explored the fitness consequences of pyoverdine sharing. This is important because experiments in shaken batch cultures repeatedly revealed that non-producers can outcompete producers, as they do not pay the cost of pyoverdine production, yet still reap the benefits of the siderophores produced by others, a phenomenon that is called "cheating" (Griffin et al. 2004; Freya Harrison et al. 2006; West, Griffin, et al. 2007; Kümmerli et al. 2010; Ghoul et al. 2014). Is cheating also possible when bacteria grow as surface-attached microcolonies? To answer this question, we grew *mcherry*-tagged producers and *gfp*-tagged non-producers in mono and mixed culture and followed microcolony growth dynamics over five hours (Figure 3). Control experiments in iron-supplemented media revealed that all strains grew equally well regardless of whether they grew in mono or mixed cultures (Figure S2). In iron-limited media, however, we found that microcolonies of non-producers grew significantly slower (t-test: t_{23}= -10.57, $p < 0.001$, Figure 3E) in monoculture and to lower cell numbers (t_{23}= -10.27, $p < 0.001$, Figure 3G) than microcolonies of producers. This shows that pyoverdine non-producers experience severe growth disadvantages when grown alone, as they are unable to efficiently scavenge iron.

This fitness pattern diametrically flipped in mixed cultures, where non-producer microcolonies grew significantly faster (t_{35}= 2.64, $p = 0.012$, Figure 3F) and to higher cell numbers (t_{31} = 2.48, $p = 0.019$, Figure 3H) than producer microcolonies. Intriguingly, non-producers experienced a relative fitness advantage between hours one and three (t-test: t_{20} = 4.53, $p < 0.001$), but not at later time points (t_{22} = 4.46, $p < 0.001$; Figure S3). This specific period at which the relative fitness benefit manifests perfectly matches the timeframe during which producers exhibited highest *pvdA* expression levels and non-producers started accumulating pyoverdine in the

periplasma (Figure 2). Our findings thus provide a direct temporal link between the high costs of pyoverdine investment to producers, the increased benefits accruing to non-producers, and the resulting opportunity for non-producers to act as cheaters and to successfully outcompete producers.

The physical boundaries of pyoverdine sharing and benefits for non-producers

The above experiments revealed that pyoverdine can be shared between two physically separated microcolonies when grown in the same field of view (128 x 96 µM) under the microscope (average ± SD distance between cells in our experiments was 36.2 ± 18.2 µM) . Next, we asked what the physical limit of pyoverdine sharing is. We thus repeated to above experiment, but this time we focussed on non-producer cells that had no producer cell within the same field of view, but only a more distant producer in an adjacent field of view (minimal distance ~ 100 µM). When examining the number of doublings taking place over five hours, we found that non-producers benefited from the presence of more distant producers in the same way as they benefited from the presence of a close producer (Figure 4A+B; significantly increased growth of non-producers in mixed culture, t-test: $t_{14} = 4.81$, $p < 0.001$). However, contrary to the previous observation (Figure 4A), the producer in mixed culture no longer experienced a significant growth reduction when non-producers were further away (Figure 4B, $t_{20} = -1.34$, $p = 0.194$).

We then expanded the distance between non-producers and producers even further by adding the two strains on opposite ends of a double-sized agarose pad. In contrast to the previous results, these assays revealed that non-producers had significantly lower number of doublings in both mixed ($t_{25} = -2.97$, $p = 0.006$) and monocultures ($t_7 = -4.11$, $p = 0.004$) (Figure 4C),

showing that pyoverdine diffusion and sharing is disabled across this large distance in the timeframe analysed.

In addition, our microscopy experiment revealed that pyoverdine sharing did not only affect the doubling rate of cells but also their size (Figure 5). Specifically, while non-producer cells were significantly smaller than producer cells in monoculture (LM: $F_{1,1294} = 150.90$, $p < 0.001$, measured three hours post-incubation), the cell size of non-producers significantly increased when grown together with a nearby producing neighbour (same field of view: $t_{446} = 10.24$, $p < 0.001$, Figure 5A; adjacent field of view: $t_{161} = 4.10$, $p < 0.001$, Figure 5B), but not when producers were far away ($t_{263} = 0.45$, $p = 0.660$, Figure 5C).

While the above experiments examined pyoverdine sharing on 1% agarose pads – a solid yet still moist environment – mimicking natural conditions as for instance encountered in moist soils or soft tissues in infections, we were wondering whether pyoverdine sharing is also possible on much harder and drier surfaces. To test this possibility, we repeated the growth experiments on 2% agarose pads. Under these conditions, we observed that non-producers no longer benefited from growing next to a producer (no significant difference in the number of doublings between mono and mixed culture: $t_{14} = -0.40$, $p = 0.693$) (Figure 6). This finding is compatible with the view that molecule diffusion is much reduced on very hard surfaces, preventing pyoverdine sharing between adjacent microcolonies.

Discussion

Our single-cell analysis on pyoverdine production in *P. aeruginosa* provides several novel insights on the social interaction dynamics between surface-attached bacteria. First, we found that pyoverdine secreted by producer cells is taken up by physically separated non-producer

cells, thereby directly demonstrating pyoverdine sharing. Second, we discovered that producer cells rapidly adjust pyoverdine expression levels when non-producers are nearby, by first up-regulating and then down-regulating pyoverdine investment. Third, we demonstrate that pyoverdine sharing has fitness consequences, as it boosts the growth and cell size of non-producers when growing in the vicinity of producers. Finally, we explored the physical limits of pyoverdine sharing and show that on soft surfaces, pyoverdine can be shared across a considerably large scale (at least 100 µM, i.e. 50 times the length of a bacterium), whereas efficient sharing is impeded with larger distances between cells and on hard surfaces. Altogether, our experiments suggest that public goods sharing and exploitation can take place between surface-attached bacteria across a wide range of naturally relevant conditions, and is mediated by molecule diffusion without the need for direct cell-to-cell contact.

Our results oppose previous work claiming that pyoverdine is predominantly shared between adjacent cells within the same microcolony (Julou et al. 2013). This claim has provoked a controversy on whether pyoverdine, and secreted compounds in general, can indeed be regarded as public goods (Zhang and Rainey 2013; Kümmerli and Ross-Gillespie 2013). The difference between our experiments and the ones performed by Julou et al. (2013) is that their study solely examined pyoverdine content of cells within the same microcolony. Unlike in our study, there was no direct test of whether pyoverdine diffuses to neighbouring microcolonies and what the fitness consequences of such diffusion would be. While we agree that a considerable amount of pyoverdine is probably shared within the microcolony, we here demonstrate that a significant amount of this molecule also diffuses out of the microcolony, providing significant growth benefits to physically separated neighbouring microcolonies. Thus, our work concisely resolves the debate by showing that secreted hydrophilic compounds, such as pyoverdine (Kümmerli et al. 2014), can be considered as public goods, even in structured environments, with the amount

of sharing and the associated fitness consequences being dependent on the distance between neighbouring microcolonies. Moreover, the distance effect we report here at the single-cell level is in line with density effects described at the community level, where secreted compounds are predominantly shared and become exploitable at higher cell densities (i.e. when individual cells are presumably closer to one another Greig and Travisano 2004; Ross-Gillespie et al. 2009; van Gestel et al. 2014; Scholz and Greenberg 2015).

A key advantage of single-cell analyses is that it allows the tracking of bacterial behavioural and growth changes in real time with high precision, immediately after the start of an experiment. This contrasts with batch culture experiments, where responses can only be measured after several hours, once the proxies for responses (e.g. optical density) become detectable at the community level. For instance, results from previous batch-culture studies suggest that pyoverdine producers seem to overinvest in pyoverdine when grown together with non-producers (Kümmerli, Jiricny, et al. 2009; Harrison 2013). However, the interpretation of these results based upon a number of assumptions, and the batch-culture approach precluded an in-depth analysis of the temporal pattern of such overinvestment and the associated fitness consequences. Our analysis now provides a nuanced view on the interactions between producers and non-producers. Specifically, we could show that soon after the inoculation of bacteria on the agarose pad, producers started overexpressing pyoverdine (Figure 2), which coincided with pyoverdine accumulation in non-producer cells (Figure 1), and significant fitness advantages to non-producers (Fig S3). Moreover, we discovered that producers can apparently respond to exploitation by non-producers by down-regulating pyoverdine production at later time points (between three and five hours), a response that correlated with the abolishment of further fitness advantages to non-producers. Thus, our results provide direct evidence for sophisticated regulatory responses to changes in the social environment, and

254 highlight that regulatory shifts and associated fitness consequences manifest much faster than previously thought.

256

Our considerations above raise questions regarding the regulatory mechanisms involved in 258 controlling the observed expression changes. Molecular studies suggest that pyoverdine is not only a siderophore, but also serves as a signalling molecule regulating its own production 260 (Beare et al. 2002; Lamont et al. 2002). Specifically, when iron-loaded pyoverdine binds to its cognate receptor FpvA, a signalling cascade is triggered, which results in the release of PvdS 262 (the iron-starvation sigma factor, initially bound to the inner cell membrane by the anti-sigma factor FpvR). PvdS then upregulates pyoverdine production. This positive feedback, triggered 264 by successful iron uptake, is opposed by a negative feedback operated by Fur (ferric uptake regulator), which silences pyoverdine synthesis once enough iron has been taken up (Ochsner 266 and Vasil 1996; Visca et al. 2007). Our results can be interpreted in the light of these feedbacks, given that the relative strength of the opposing feedbacks determines the resulting pyoverdine 268 investment levels (Weigert et al. 2017). When growing in monoculture, producer cells can efficiently share pyoverdine, which supposedly stimulates both pyoverdine-signalling and iron 270 uptake. Positive and negative feedback should thus be in balance and result in an intermediate pyoverdine investment levels. Conversely, when producers grow in mixed cultures then non-272 producers serve as a sink for pyoverdine, and reduce iron supply to producers. In this scenario, the positive feedback should be stronger than the negative feedback, resulting in the 274 upregulation of pyoverdine. While these elaborations are compatible with the pyoverdine expression patterns at hour one and three in our experiment, the flip in expression patterns 276 between mono and mixed cultures observed after five hours is more difficult to explain. One option would be that the previously described switch from pyoverdine production to recycling 278 (Faraldo-Gómez and Sansom 2003; Imperi et al. 2009; Kümmerli and Brown 2010) occurs

earlier in mixed than in monocultures. An alternative and more exciting option would be that producers can recognize the presence of exploitative cheaters and downscale their cooperative efforts accordingly.

Our results showing that non-producers can outcompete producers in mixed cultures, even when microcolonies are physically separated, confirms predictions from social evolution theory for microbes (Allison 2005; West et al. 2006; Driscoll and Pepper 2010; Dobay et al. 2014). One key condition required for cooperation to be maintained is that cooperative acts must more often be directed towards other cooperators than expected by chance. This interaction probability is measured as the degree of relatedness *r*, a parameter central to inclusive fitness theory (Hamilton 1964; Frank 1998). Traditionally, high relatedness has been associated with the physical separation of cooperators and non-cooperators into distinct patches (Frank 1998). Our results now show that this traditional view is not applicable to public goods cooperation in bacteria, because the physical separation of pyoverdine producer and non-producer colonies is insufficient to maintain cooperation and prevent exploitations by non-producers (Figure 3). Clearly, relatedness in our scenario should be measured at the scale at which pyoverdine sharing can occur (West et al. 2006), which largely exceeds the boundaries of a single microcolony. Thus, in scenarios where microbial cells are immobile, it is the diffusion properties of the public good that determines the degree of relatedness between interacting partners.

In summary, our finding on pyoverdine sharing and exploitation between physically separated microcolonies has broad implications for our understanding of the social life of bacteria in many natural settings. This is because bacteria typically live in surface-attached communities in aquatic and terrestrial ecosystems, as well as in infections (Nadell et al. 2009; Flemming et al. 2016). Many of these natural habitats feature soft surfaces, as mimicked by our experimental

304 set up, making the diffusion and sharing of secreted compounds between cells highly likely. However, our work also revealed physical limits to public goods cooperation, namely on hard 306 surfaces, where public good diffusion and sharing is impeded. This shows that whether or not a secreted compound is shared is context-dependent (Kümmerli et al. 2014), and relies, amongst 308 other factors, on the physical properties of the environment.

310 Materials and methods

Strains and media

312 Our experiments featured the clinical isolate *P. aeruginosa* PAO1 (ATCC 15692), and its clean deletion knock-out mutant of pyoverdine, directly derived from this wildtype (PAO1*ΔpvdD*). 314 To be able to distinguish the two strains under the microscope, we engineered fluorescent variants of these strains via chromosomal insertion (*att*Tn7::ptac-*gfp*, *att*Tn7::ptac-*mcherry*) – 316 i.e. PAO1-*gfp*, PAO1-*mcherry*, PAO1Δ*pvdD-gfp* and PAO1Δ*pvdD-mcherry*. A preliminary experiment revealed that these fluorescent markers did not affect the growth performance of 318 the strains (Figure S2). For our gene expression experiments, we used the reporter strain PAO1*pvdA-gfp* (chromosomal insertion: *att*B::*pvdA-gfp)* (Kaneko et al. 2007). PvdA catalyses 320 an important step in the biosynthesis pathway of pyoverdine (Leoni et al. 1996), and its expression level is therefore a good proxy for the investment into pyoverdine production.

322

Overnight cultures were grown in 8 ml Lysogeny Broth (LB) medium in 50 ml Falcon tubes, 324 and incubated at 37°C, 200 rpm for 16-18 hours. Cells were then harvested by centrifugation at 3000 rpm for 3 minutes and resuspension in 8 ml of 0.8% NaCl (saline solution). For all 326 experiments, we subsequently diluted the washed cultures in saline solution to an OD = 1 (optical density at 600 nm). For all microscopy experiments, we used CAA medium (per liter: 328 5 g casamino acids, 1.18 g K_2HPO_4*$3H_2O$, 0.25 g $MgSO_4$*$7H_2O$, 450). To create severe iron

limitation, we added the chemical iron chelator 2,2-Bipyridin (final concentration 450 µM). To create iron-replete conditions, we added 200 µM $FeCl_3$. All chemicals were purchased from Sigma-Aldrich (Buchs SG, Switzerland).

Preparation of microscopy slides

We adapted a method previously described in (de Jong et al. 2011). Standard microscopy slides (76 mm x 26 mm) were washed with EtOH and dried in a laminar flow. We used 65 µL "Gene Frames" (Thermo Fisher Scientific) to prepare agarose pads. Each frame features a single chamber of 0.25 mm thickness (1.5 x 1.6 cm) and 65 µl volume. The frame is coated with adhesives on both sides so that it sticks to the microscopy slide, and at the same time adheres the cover glass from the top. The sealed chamber is airproof, which is necessary to prevent evaporation and deformation of the pad during the experiment.

To prepare microscopy pads, we heated 20 mL CAA supplemented with agarose (1% unless indicated otherwise) in a microwave. The melted agarose-media mix was subsequently cooled to approximately 50°C. Next, we added the supplements: either 2,2-Bipyridin (final concentration 450 µM) or $FeCl_3$ (final concentration 200 µM) to create iron-limited or iron-replete conditions, respectively. We pipetted 360 µL of the agarose solution into the gene frame and immediately covered it with a cover glass. The cover glass was pressed down with a gentle pressure to dispose superfluous media. After the solidification of the agarose pad (ca. 30 minutes), we removed the cover glass (by carefully sliding it sideways) and divided the original pad into 4 smaller pads of equal size by using a sterile scalpel. The further introduced channels between pads, which served as a reservoir for oxygen. We then put 1 µL of highly diluted bacterial culture (OD = 1 cultured diluted by $2.5*10^{-4}$) in the middle of each pad. Two pads were inoculated with a 1:1 mix of pyoverdine producers and non-producers, whereas the other

two pads were inoculated with a monoculture (either producer or non-producer). After the inoculum drop had evaporated, we sealed the pads with a new cover glass using the adhesive of the Gene Frame. With this protocol, we managed to create agarose pads with consistent properties across experiments.

Microscopy setup and imaging

All experiments were carried out at the Center for Microscope and Image Analysis of the University Zürich (ZMB) using a widefield Leica DMI6000 microscope. The microscope featured a plan APO PH3 objective (NA = 1.3), an automated stage and an auto-focus. For fluorescent imaging, we used a Leica L5 filter cube for GFP (Emission: 480 ± 40 nm, Excitation: 527 ± 30 nm, DM = 505) and a Leica TX2 filter cube for mCherry (Emission: 560 ± 40 nm, Excitation: 645 ± 75 nm, DM = 595). Auto-fluorescence of pyoverdine was captured with a Leica CFP filter cube (Emission: 436 ± 20 nm, Excitation: 480 ± 40 nm, DM = 455). We used a Leica DFC 350 FX camera (resolution: 1392x1040 pixels) for image recording (16 bit colour depth).

Image processing and blank subtraction

To extract information (cell size, fluorescence) from every single cell, images had first to be segmented. Segmentation is the process of dividing an image into objects and background. Since it is currently a bottleneck for high throughput image analysis (Van Valen et al. 2016), we developed a new workflow (detailed protocol available upon request). This workflow includes a protocol for the rapid, reliable and fully automated image segmentation without the need for any priors (i.e. information on cell size and shape) and manual corrections. The workflow starts with the machine learning, supervised object classification and segmentation tool ilastik (Sommer et al. 2011). Ilastik features a self-learning algorithm that autonomously

explores the parameter space for object recognition. We used a low number of phase contrast images from our experiments to train ilastik for bacterial cell recognition and segmentation. Each training round is followed by user inputs regarding segmentation errors. These inputs are then incorporated in the next training round, until segmentation is optimized and error-free. Once the training is completed, microscopy images from all experiments can be fed to ilastik and segmentation is then carried out in a fully automated manner, without the need for any further manual corrections. Ilastik produces binary images as an output (black background vs. white objects).

For image analysis, this output was then transferred to Fiji, a free scientific image processing software package (Schindelin et al. 2012). We wrote specific macro-scripts in Fiji to fully automate the simultaneous analysis of multiple single-cell features such as cell size, shape, fluorescence, etc. First, we used the binary images to create an overlay of the region of interests for every single cell, which could then be used in a second step to measure bacterial properties from phase contrast and fluorescence images (see supplementary material for a step-by-step protocol). Next, we applied a pixel-based blank correction procedure in Fiji, to obtain unbiased fluorescence intensities for each cell. For each agarose pad and time point, we imaged four empty random positions on the agarose pad without bacterial cells and averaged the grey values for each pixel. The averaged grey value of each pixel was than subtracted from the corresponding pixel position in images containing cells. This pixel-based blank correction accounts for intensity differences across the field of view caused by the optical properties of the microscope (vignetting). In the experiments where we simultaneously measured *pvdA-gfp* expression and pyoverdine fluorescence, we had to further correct for the leakage of pyoverdine signal into the GFP-channel. To do so, we imaged cells of the unmarked wildtype strain, which produced pyoverdine but had no GFP reporter. We then measured the pyoverdine signal in the

GFP-channel at three different time points (one, three and five hours post-incubation), and then used these values to blank correct the fluorescence intensities in cells with the *pvdA*-GFP reporter.

Assays measuring *pvdA* expression and pyoverdine fluorescence

To monitor pyoverdine investment by producer cells and pyoverdine uptake by non-producer cells, we quantified natural pyoverdine fluorescence in bacterial micro-colonies of both strains in mixed and monocultures over time. For producer micro-colonies we further measured *pvdA* expression levels over time. Because the excitation wavelength for pyoverdine fluorescence overlaps with the UV range, the high exposure time required to measure natural pyoverdine fluorescence induces damage (i.e. phototoxicity) to bacterial cells. Accordingly, each bacterial micro-colony could only be measured once. To obtain time course data for pyoverdine expression and uptake levels, we thus prepared multiple microscopy slides, as described above, and incubated them at 37 °C in a static incubator. At each time step (one, three and five hours post incubation), we then processed two slides for imaging. Exposure time for measuring gfp-fluorescence was 800 ms and for pyoverdine 1500 ms, with a (halogen) lamp intensity of 100%. To guarantee reliable automated image analysis, we only considered positions that were free from non-bacterial objects (e.g. dust) and where all cells laid within one focus layer. Focus was adjusted manually. We recorded at least five positions per treatment, time point and slide. The experiment was carried out twice, in two completely independent batches.

Fitness assays

We used time-laps microscopy to measure the growth performance of pyoverdine producer cells (tagged with mCherry) and non-producer cells (tagged with GFP) in mixed and monoculture. As described above, we cut the agarose pad in four patches and inoculated two

patches with a 1:1 mix of producers and non-producers, and one patch each with a monoculture. We then chose 20 positions (five per patch) that contained two separated cells (one cell of each strain for mixed cultures and two cells of the same type for monocultures), and imaged these positions sequentially every 15 minutes over 5 hours, using the automated stage function of the microscope. Following a position change and prior to imaging, we used the auto-focus function of the microscope to adjust the z-position in order to keep cells in focus. This protocol allowed us to follow the growth of micro-colonies from a single-cell stage.

We carried out the above fitness assays across a range of different conditions. In a control experiment, we added 200 µM $FeCl_3$ to the agarose pad to study the strain growth in the absence of iron limitation. Since bacteria grow very well in iron-replete media, we stopped the imaging after three hours before micro-colonies started to grow in multiple layers. Next, we monitored strain growth on iron-limited 1% agarose pads supplemented with 450 µM bipyridin. To examine whether pyoverdine sharing and fitness effects depend on the distance between two cells, we performed fitness assays where two cells were positioned: (i) close to one another in the same field of view (average distance between cells 36.21 µM ± 18.17 SD) ; (ii) further apart in adjacent fields of view (with an estimated minimum distance of 96 µm, given the field of view size of 96 x 128 µm); and (iii) far from one another. This latter condition was created by adding the two strains on opposite ends of an elongated double-sized agarose pad. Finally, we repeated the growth assays in media with increased viscosity (i.e. on 2 % agarose pads).

Statistical methods

All statistical analyses were performed in R 3.3.0 (R Development Core Team 2015) using linear models (ANOVA or t-tests). Prior to analysis, we used the Shapiro-Wilk test to check whether model residuals were normally distributed. Since each experiment was carried out in

multiple independent experimental blocks, we scaled values within each block relative to the mean of the control treatment (i.e. pyoverdine producer grown in monoculture). For all time-laps growth experiments, we considered the position (i.e. the field of view) as the level of replication. This is justified because we chose positions on the same pad that were far apart to guarantee independence. For the analysis of single cell fluorescence data, we considered each cell as a replicate.

Acknowledgments

We thank Urs Ziegler and Caroline Aemisegger for help with the microscope, Moritz Kirschmann for advice regarding single cell data analysis, and the SNSF (grant no. PP00P3_165835 to RK), the ERC (grant no. 681295 to RK) and the DAAD (to MW) for funding.

Funding statement

Funding organisations had no influence on study design, data collection and interpretation or the decision to submit the work for publication.

Data Archiving Statement

Upon acceptance, raw data and scripts will be made available on Dryad.

Competing interests

None declared.

Contributions

Conception and design by MW and RK, Acquisition of data by MW, Analysis and interpretation of data by MW and RK, Drafting and revising the article by MW and RK.

References

Alizon, S., S. Lion. 2011. Within-host parasite cooperation and the evolution of virulence. Proceedings of the Royal Society B: Biological Sciences 278: 3738–47.

Allison, S. D. 2005. Cheaters, diffusion and nutrients constrain decomposition by microbial enzymes in spatially structured environments. Ecology Letters 8: 626–35.

Bachmann, H., F. J. Bruggeman, D. Molenaar, F. Branco dos Santos, B. Teusink. 2016. Public goods and metabolic strategies. Current Opinion in Microbiology 31: 109–15.

Beare, P. A., R. J. For, L. W. Martin, I. L. Lamont. 2002. Siderophore-mediated cell signalling in *Pseudomonas aeruginosa*: divergent pathways regulate virulence factor production and siderophore receptor synthesis. Molecular Microbiology 47: 195–207.

Buckling, A., F. Harrison, M. Vos, M. a Brockhurst, A. Gardner, S. a West, A. Griffin. 2007. Siderophore-mediated cooperation and virulence in *Pseudomonas aeruginosa*. FEMS Microbiology Ecology 62: 135–41.

de Jong, I. G., K. Beilharz, O. P. Kuipers, J.-W. Veening. 2011. Live cell imaging of *Bacillus subtilis* and *Streptococcus pneumoniae* using automated time-lapse microscopy. Journal of Visualized Experiments, no. 53.

Dobay, A., H. C. Bagheri, A. Messina, R. Kümmerli, D. J. Rankin. 2014. Interaction effects of cell diffusion, cell density and public goods properties on the evolution of cooperation in

digital microbes. Journal of Evolutionary Biology 27: 1869–77.

Drescher, K., C. D. Nadell, H. A. Stone, N. S. Wingreen, B. L. Bassler. 2014. Solutions to the public goods dilemma in bacterial biofilms. Current Biology 24: 50–55.

Driscoll, W. W., J. W. Pepper. 2010. Theory for the evolution of diffusible external goods. Evolution; International Journal of Organic Evolution 64: 2682–87.

Faraldo-Gómez, J. D., M. S. P. Sansom. 2003. Acquisition of siderophores in Gram-negative bacteria. Nature Reviews Molecular Cell Biology 4: 105–16.

Flemming, H.-C., J. Wingender, U. Szewzyk, P. Steinberg, S. A. Rice, S. Kjelleberg. 2016. Biofilms: an emergent form of bacterial life. Nature Reviews Microbiology 14: 563–75.

Foster, K. R., T. Bell. 2012. Competition, not cooperation, dominates interactions among culturable microbial species. Current Biology : CB 22: 1845–50.

Frank, S. A. 1998. Foundations of Social Evolution. Princeton University Press

Ghoul, M., S. A. West, S. P. Diggle, A. S. Griffin. 2014. An experimental test of whether cheating is context dependent. Journal of Evolutionary Biology 27: 551–56.

Greig, D., M. Travisano. 2004. The Prisoner's Dilemma and polymorphism in yeast SUC genes. Proceedings of the Royal Society B: Biological Sciences 271: S25–26.

Griffin, A. S., S. A. West, A. Buckling. 2004. Cooperation and competition in pathogenic bacteria. Nature 430.

Hamilton, W. D. 1964. The genetical evolution of social behaviour. Journal of Theoretical Biology 7: 1–52.

Harrison, F. 2013a. Dynamic social behaviour in a bacterium: *Pseudomonas aeruginosa*

partially compensates for siderophore loss to cheats. Journal of Evolutionary Biology 26: 1370–78.

Harrison, F. 2013b. Social versus nonsocial cues and responses: a reply to Alizon. Journal of Evolutionary Biology 26: 2297–98.

Harrison, F., L. E. Browning, M. Vos, A. Buckling. 2006. Cooperation and virulence in acute *Pseudomonas aeruginosa* infections. BMC Biology 4: 21.

Imperi, F., F. Tiburzi, P. Visca. 2009. Molecular basis of pyoverdine siderophore recycling in Pseudomonas aeruginosa. Proceedings of the National Academy of Sciences of the United States of America 106: 20440–45.

Inglis, R. F., J. M. Biernaskie, A. Gardner, R. Kümmerli. 2016. Presence of a loner strain maintains cooperation and diversity in well-mixed bacterial communities. Proceedings of the Royal Society B: Biological Sciences 283: 20152682.

Jousset, A., N. Eisenhauer, E. Materne, S. Scheu. 2013. Evolutionary history predicts the stability of cooperation in microbial communities. Nature Communications 4: 2573.

Julou, T., T. Mora, L. Guillon, V. Croquette, I. J. Schalk, D. Bensimon, N. Desprat. 2013. Cell-cell contacts confine public goods diffusion inside *Pseudomonas aeruginosa* clonal microcolonies. Proceedings of the National Academy of Sciences of the United States of America 110: 12577–82.

Kaneko, Y., M. Thoendel, O. Olakanmi, B. E. Britigan, P. K. Singh. 2007. The transition metal gallium disrupts *Pseudomonas aeruginosa* iron metabolism and has antimicrobial and antibiofilm activity. Journal of Clinical Investigation 117: 877–88.

Köhler, T., A. Buckling, C. van Delden. 2009. Cooperation and virulence of clinical

546 *Pseudomonas aeruginosa* populations. Proceedings of the National Academy of Sciences 106: 6339–44.

548 Kümmerli, R., S. P. Brown. 2010. Molecular and regulatory properties of a public good shape the evolution of cooperation. Proceedings of the National Academy of Sciences of the United 550 States of America 107: 18921–26.

Kümmerli, R., A. Gardner, S. A. West, A. S. Griffin. 2009. Limited dispersal, budding 552 dispersal, and cooperation: an experimental study. Evolution; International Journal of Organic Evolution 63: 939–49.

554 Kümmerli, R., N. Jiricny, L. S. Clarke, S. A. West, A. S. Griffin. 2009. Phenotypic plasticity of a cooperative behaviour in bacteria. Journal of Evolutionary Biology 22: 589–98.

556 Kümmerli, R., A. Ross-Gillespie. 2013. Explaining the Sociobiology of Pyoverdin Producing *Pseudomonas*: a Comment on Zhang and Rainey (2013). Evolution; International Journal of 558 Organic Evolution, 1–7.

Kümmerli, R., K. T. Schiessl, T. Waldvogel, K. McNeill, M. Ackermann. 2014. Habitat 560 structure and the evolution of diffusible siderophores in bacteria. Ecology Letters 17: 1536–44.

562 Kümmerli, R., P. van den Berg, A. Griffin, S. A. West, A. Gardner. 2010. Repression of competition favours cooperation: experimental evidence from bacteria. Journal of 564 Evolutionary Biology 23: 699–706.

Lamont, I. L., P. A. Beare, U. Ochsner, A. I. Vasil, M. L. Vasil. 2002. Siderophore-mediated 566 signaling regulates virulence factor production in *Pseudomonas aeruginosa*. Proceedings of the National Academy of Sciences 99: 7072–77.

568 Leinweber, A., R. Fredrik Inglis, R. Kümmerli. 2017. Cheating fosters species co-existence in well-mixed bacterial communities. The ISME Journal, January.

570 Leoni, L., A. Ciervo, N. Orsi, P. Visca. 1996. Iron-regulated transcription of the pvdA gene in *Pseudomonas aeruginosa*: effect of Fur and PvdS on promoter activity. Journal of
572 Bacteriology 178: 2299–2313.

Miethke, M., M. A. Marahiel. 2007. Siderophore-based iron acquisition and pathogen control.
574 Microbiology and Molecular Biology Reviews 71: 413–51.

Nadell, C. D., B. L. Bassler. 2011. A fitness trade-off between local competition and dispersal
576 in *Vibrio cholerae* biofilms. Proceedings of the National Academy of Sciences of the United States of America 108: 14181–85.

578 Nadell, C. D., J. B. Xavier, K. R. Foster. 2009. The sociobiology of biofilms. FEMS Microbiology Reviews 33: 206–24.

580 Ochsner, U. A., M. L. Vasil. 1996. Gene repression by the ferric uptake regulator in Pseudomonas aeruginosa: cycle selection of iron-regulated genes. Proceedings of the National
582 Academy of Sciences of the United States of America 93: 4409–14.

Pollitt, E. J. G., S. A. West, S. A. Crusz, M. N. Burton-Chellew, S. P. Diggle. 2014.
584 Cooperation, quorum sensing, and evolution of virulence in *Staphylococcus aureus*. Infection and Immunity 82: 1045–51.

586 R Development Core Team. 2015. R: A language and environment for statistical computing.

Ratledge, C., L. G. Dover. 2000. Iron metabolism in pathogenic bacteria. Annual Review in
588 Microbiology 54: 881–941.

Ross-Gillespie, A., A. Gardner, A. Buckling, S. A. West, A. S. Griffin. 2007. Frequency dependence and cooperation: theory and a test with bacteria. The American Naturalist 170: 242–331.

Ross-Gillespie, A., A. Gardner, A. Buckling, S. A. West, A. S. Griffin. 2009. Density dependence and cooperation: theory and a test with bacteria. Evolution; International Journal of Organic Evolution 63: 2315–25.

Schalk, I. J., L. Guillon. 2013. Fate of ferrisiderophores after import across bacterial outer membranes: different iron release strategies are observed in the cytoplasm or periplasm depending on the siderophore pathways. Amino Acids 44: 1267–77.

Schindelin, J., I. Arganda-Carreras, E. Frise, V. Kaynig, M. Longair, T. Pietzsch, S. Preibisch, et al. 2012. Fiji: an open-source platform for biological-image analysis. Nature Methods 9: 676–82.

Scholz, R. L., E. P. Greenberg. 2015. Sociality in Escherichia coli: Enterochelin Is a Private Good at Low Cell Density and Can Be Shared at High Cell Density. Journal of Bacteriology 197: 2122–28.

Sommer, C., C. Strähle, U. Köthe, F. A. Hamprecht. 2011. Ilastik: Interactive Learning and Segmentation Toolkit. Eighth IEEE International Symposium on Biomedical Imaging (ISBI), 230–33.

van Gestel, J., F. J. Weissing, O. P. Kuipers, A. T. Kovács. 2014. Density of founder cells affects spatial pattern formation and cooperation in *Bacillus subtilis* biofilms. The ISME Journal 8: 2069–79.

Van Valen, D. A., T. Kudo, K. M. Lane, D. N. Macklin, N. T. Quach, M. M. DeFelice, I.

Maayan, Y. Tanouchi, E. A. Ashley, M. W. Covert. 2016. Deep Learning Automates the
612 Quantitative Analysis of Individual Cells in Live-Cell Imaging Experiments. PLOS
Computational Biology 12: e1005177.

614 Visca, P., F. Imperi, I. L. Lamont. 2007. Pyoverdine siderophores: from biogenesis to
biosignificance. Trends in Microbiology 15: 22–30.

616 Weigert, M., A. Ross-Gillespie, A. Leinweber, G. Pessi, S. P. Brown, R. Kümmerli. 2017.
Manipulating virulence factor availability can have complex consequences for infections.
618 Evolutionary Applications 10: 91–101.

West, S. A., S. P. Diggle, A. Buckling, A. Gardner, A. S. Griffin. 2007. The Social Lives of
620 Microbes. Annual Review of Ecology, Evolution, and Systematics 38: 53–77.

West, S. A., A. S. Griffin, A. Gardner. 2007. Evolutionary Explanations for Cooperation.
622 Current Biology 17: 661–72.

West, S. A., A. S. Griffin, A. Gardner, S. P. Diggle. 2006. Social evolution theory for
624 microorganisms. Nature Reviews Microbiology 4: 597–607.

Zhang, X.-X., P. B. Rainey. 2013. Exploring the Sociobiology of Pyoverdine-Producing
626 *Pseudomonas*. Evolution 67: 3161–74.

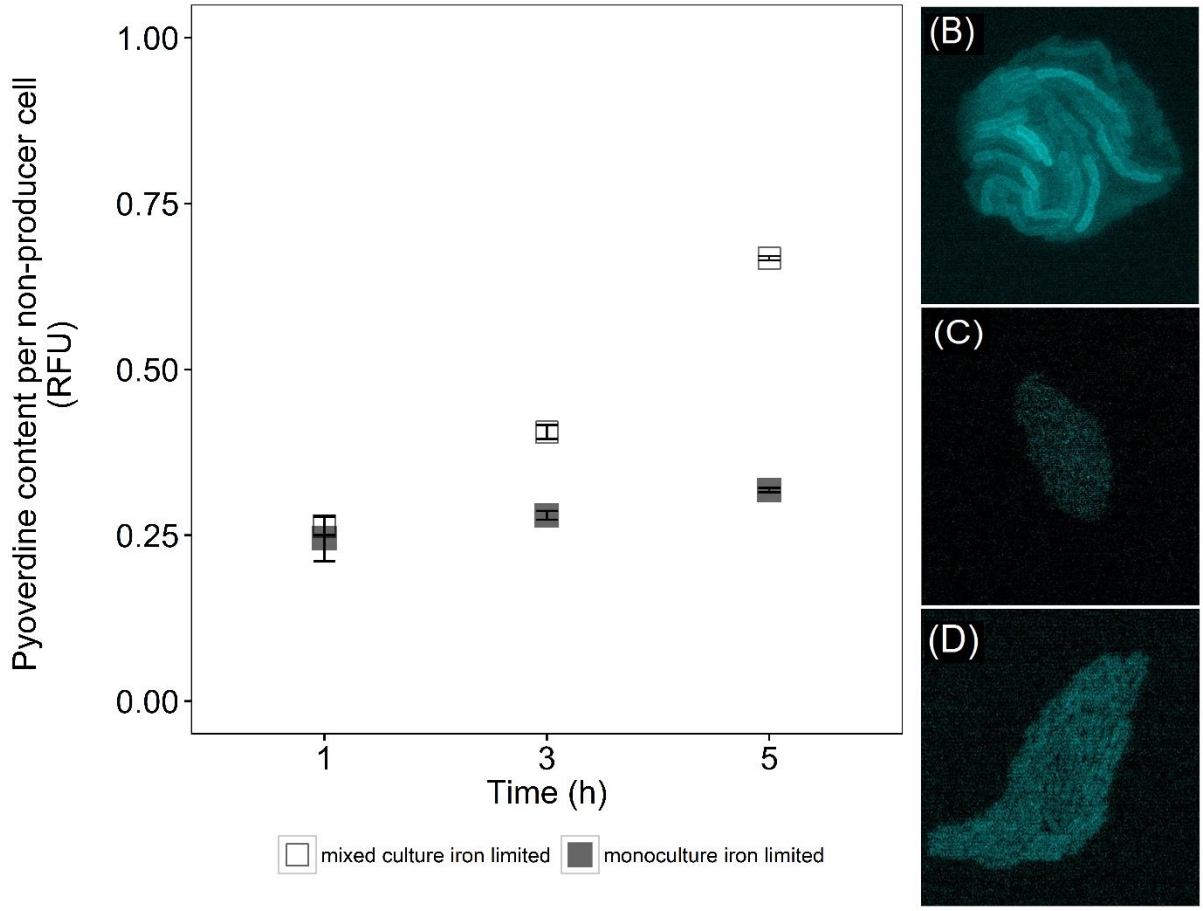

Figure 1: Pyoverdine is taken up by non-producing cells in a time-dependent manner, demonstrating pyoverdine sharing between physically separated, surface-attached micro-colonies. **(A)** Time-course measures on natural pyoverdine fluorescence units (RFU) shows constant background fluorescence in non-producer cells grown in monocultures (filled squares), whereas pyoverdine fluorescence significantly increased in non-producer cells grown in mixed cultures with producers (open squares). Mean relative fluorescence values ± standard errors are scaled relative to producer monocultures after one hour of growth. Representative microscopy pictures show pyoverdine fluorescence in a producer microcolony from a mixed culture **(B)**, a non-producer colony from a monoculture **(C)**, and a non-producer colony from a mixed culture **(D)**. Important to note is that only apo-pyoverdine (i.e. iron-free) is fluorescent, and therefore the measured fluorescence intensities represent a conservative measure of the actual pyoverdine content per cell. Furthermore, the fluorescence intensity in producer cells is always higher than in non-producer cells because it represents the sum of pyoverdine taken up from the environment and newly synthesized pyoverdine, whereas for non-producers, fluorescence represents pyoverdine uptake only.

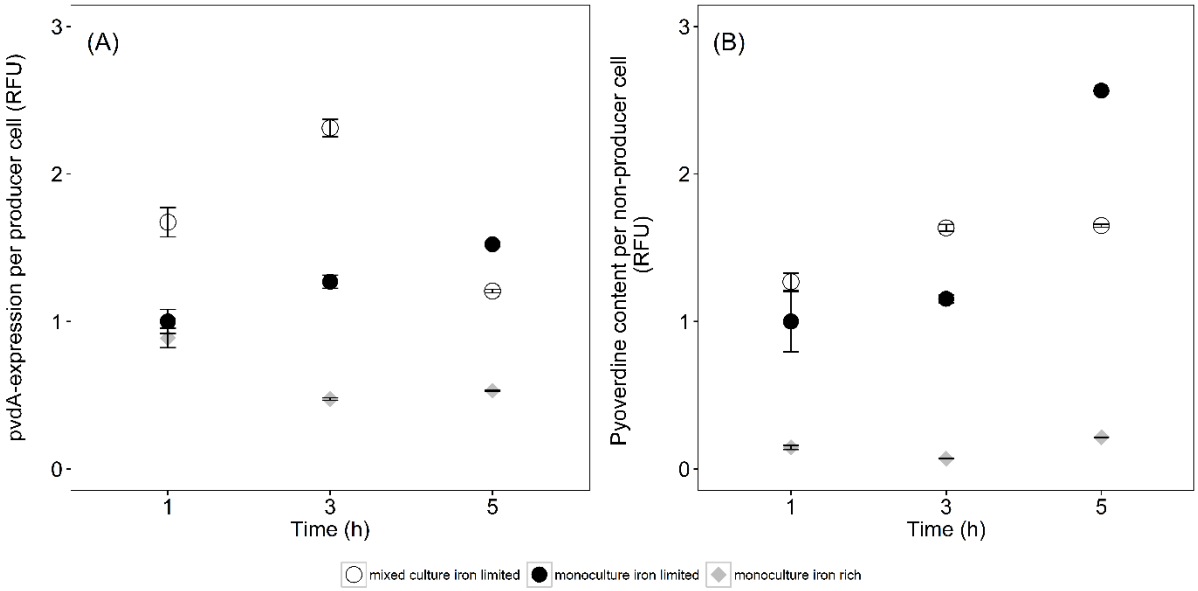

Figure 2: Producer cells adjust their pyoverdine investment level in response to changes in the social environment, supporting the view that pyoverdine is a shared signalling molecule in surface-attached microcolonies. **(A)** Time-course data show that *pvdA*, a gene encoding an enzyme involved in pyoverdin synthesis, is down-regulated in iron-rich media (grey diamonds), but up-regulated in iron-deplete media. Importantly, producers exhibited different *pvdA* expression patterns depending on whether they grew together with nonproducers (open circles) or as monoculture (filled circles). While producers showed increased gene expression in mixed compared to monoculture after one and three hours, the pattern flipped after five hours. **(B)** The same qualitative pattern was observed when measuring pyoverdine content per cell, as relative fluorescence units (RFU). Fluorescence values are scaled relative to the producer monocultures after one hour of growth. Important to note is that only apo-pyoverdine (i.e. iron-free) is fluorescent. Error bars indicate standard errors of the mean.

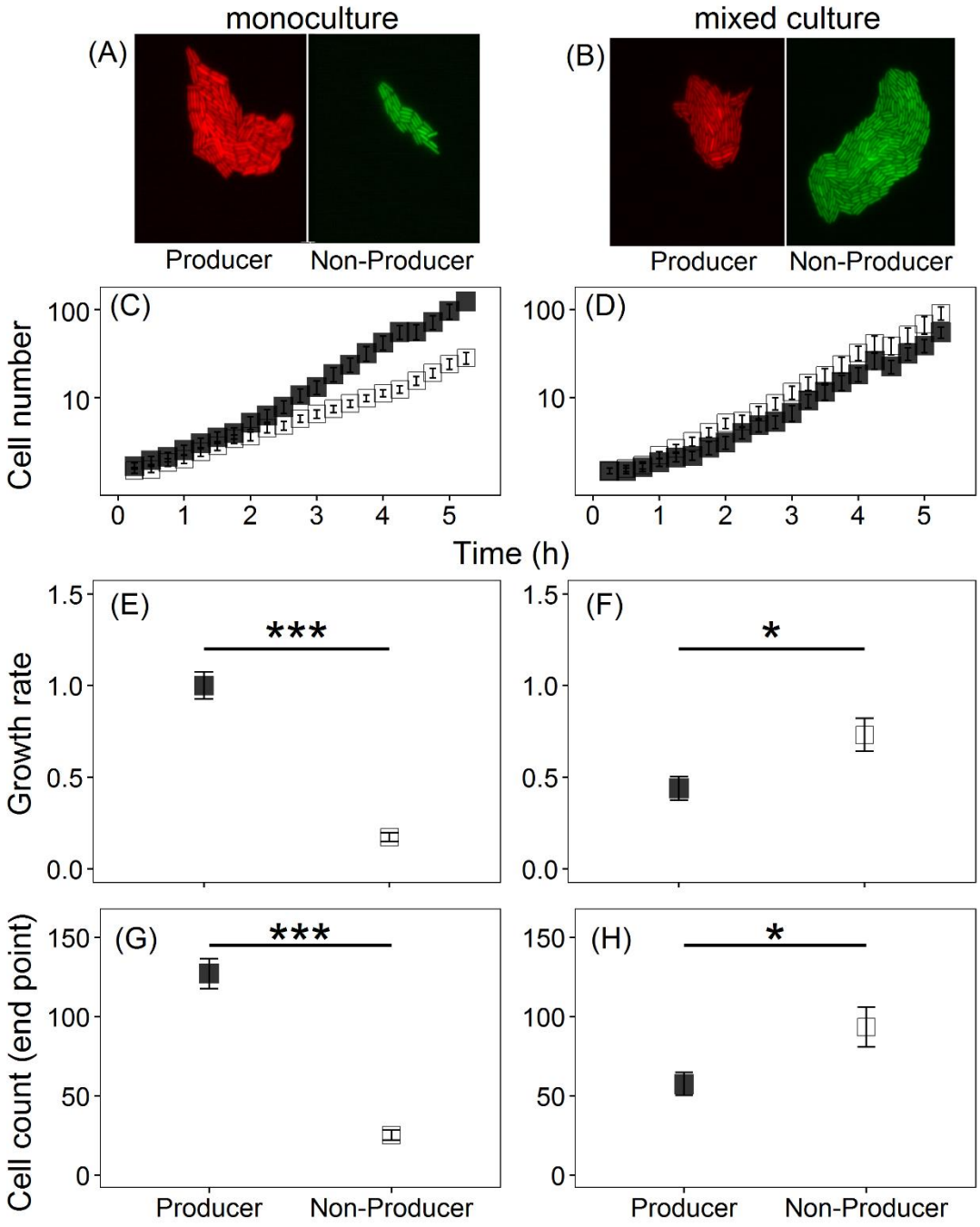

Figure 3: Growth performance of surface-attached microcolonies of pyoverdine producers (filled squares) and non-producers (open squares) in monocultures (left column) and mixed cultures (right column). While pyoverdine non-producers show growth deficiencies in monoculture, due to their inability to scavenge iron, they outcompete the producers in mixed cultures. This growth pattern shows that non-producers save costs by not making any pyoverdine, yet gain fitness benefits by capitalizing on the pyoverdine secreted by the producers. **(A)** and **(B)** show representative microscopy pictures for monocultures and mixed cultures, respectively. The overall growth trajectories of producers and non-producers differ substantially between monocultures **(C)** and mixed cultures (**D)**. While producers had a significantly higher growth rate **(E)** and grew to higher cell numbers **(G)** in monocultures, the exact opposite was the case in mixed cultures for both the growth rate **(F)** and cell number **(H)**. Growth parameters are given relative to the producers in monoculture. Asterisks indicate significant differences and error bars denote standard errors of the mean.

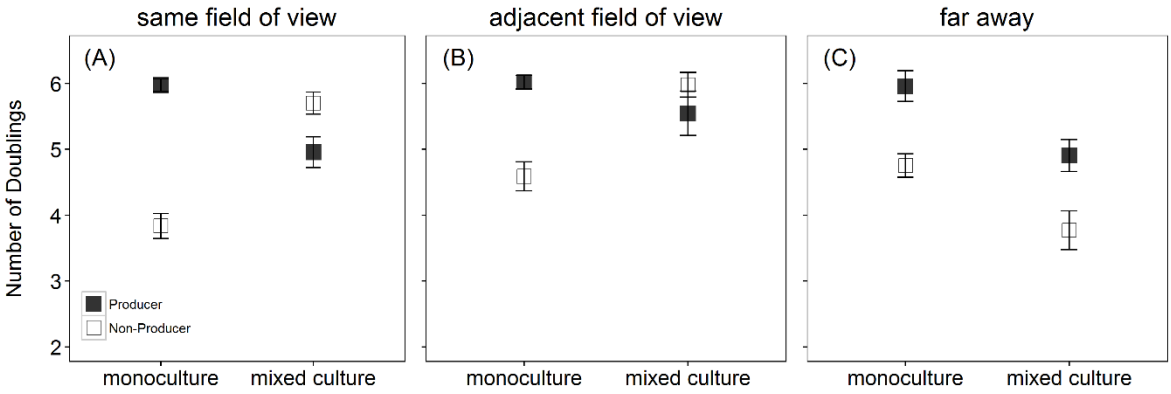

Figure 4: The relative fitness advantage of pyoverdine nonproducers in mixed cultures is dependent on the distance between producer (filled squares) and non-producer (open squares) microcolonies. In monoculture assays, the non-producers had significantly lower number of doublings than the producers in all experiments. In mixed cultures, meanwhile, the number of doublings of non-producers significantly increased when the producer microcolony was (**A**) within the same field of view (average distance between cells 36 µm), **(B)** in an adjacent field of view (minimal distance ~ 100 µm), but not when producers were far away (on opposite ends of the agarose pad) (**C**). These analyses show that pyoverdine can be shared and exploited across a relative large distance (at least 100 µm). Error bars indicate the standard error of the mean.

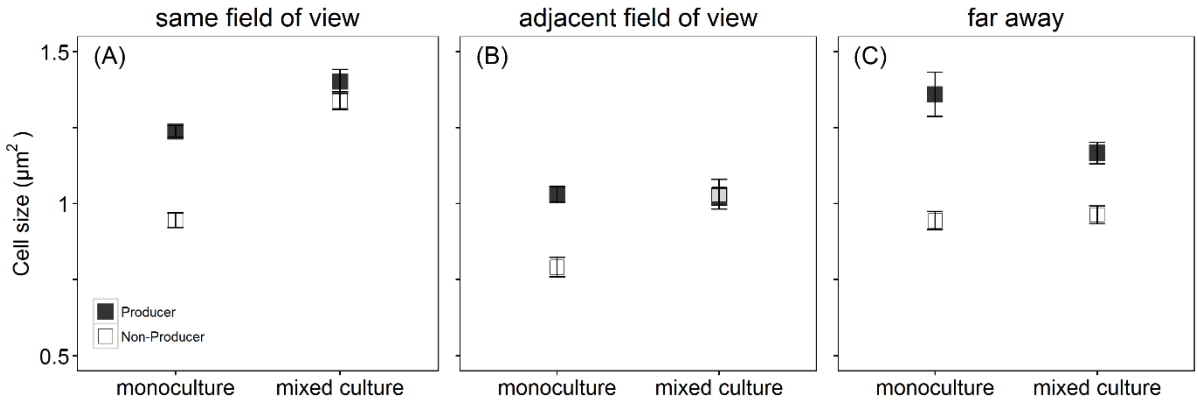

686 **Figure 5:** Pyoverdine sharing affects cell size. While non-producer cells (open squares) were
significantly smaller than producer cells (closed squares) in monocultures, non-producer cell size was
688 restored to wildtype level in mixed cultures when the producer microcolony was (**A**) within the same
field of view (average distance between cells 36 µm), **(B)** in an adjacent field of view (minimal distance
690 ~ 100 µm), but not when producers were far away (on opposite ends of the agarose pad) (**C**). Cell size
was measured after three hours of growth. Error bars indicate the standard error of the mean.

692

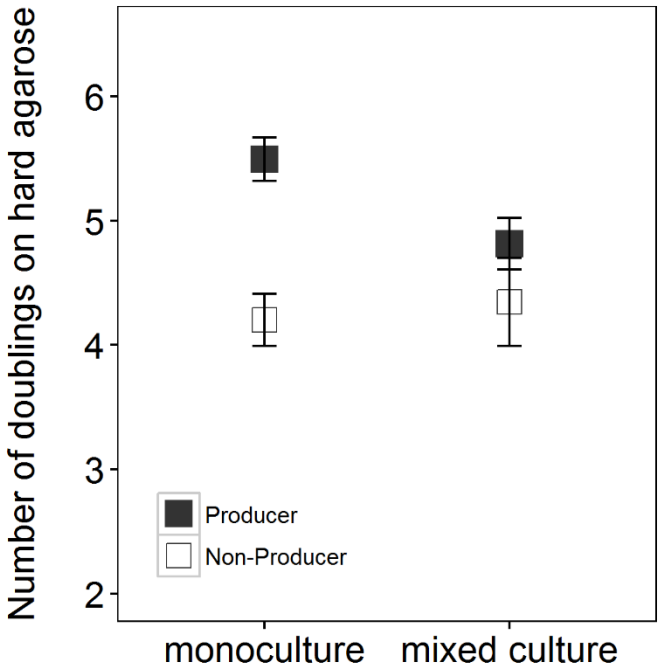

694

Figure 6: Pyoverdine sharing is impeded on hard surfaces. While the previous experiments showed that
696 pyoverdine is extensively shared between neighbouring microcolonies on relatively soft surfaces (1 %
agarose), efficient sharing was no longer possible on hard surfaces (2 % agarose). Under these latter
698 conditions, non-producers (open squares) were significantly impaired in their growth even when being
located next to producers. Error bars indicate the standard error of the mean.

700

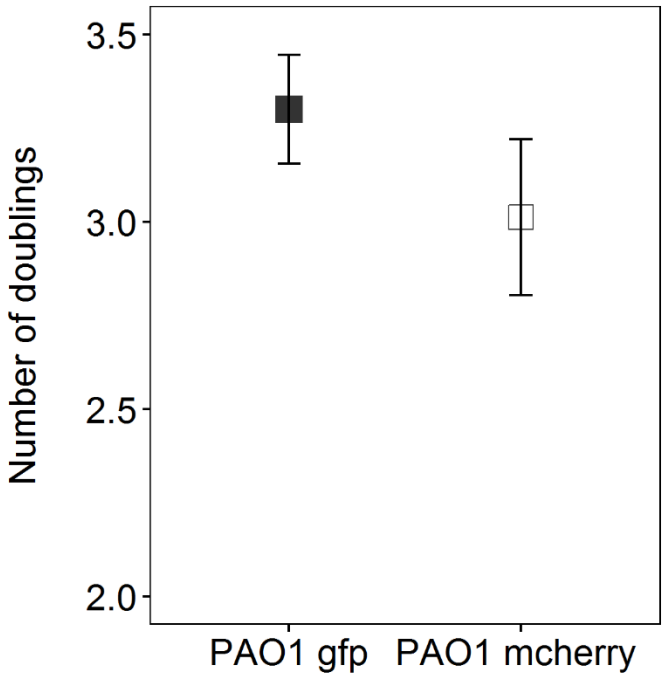

Figure S 1: Growth did not differ between strains tagged with GFP or mCherry. We grew the wildtype PAO1 strain, either tagged with GFP or mCherry on iron-limited agarose pads and calculated the number of doublings over 5 hours. Doubling numbers did not significantly differ between the two strains (t-test: $t_{94} = 1.14$, $p = 0.258$). Thus, we can be confident that growth differences observed in our experiments are due to biological and not tag effects. Symbols and error bars indicate means and standard errors of the mean, respectively.

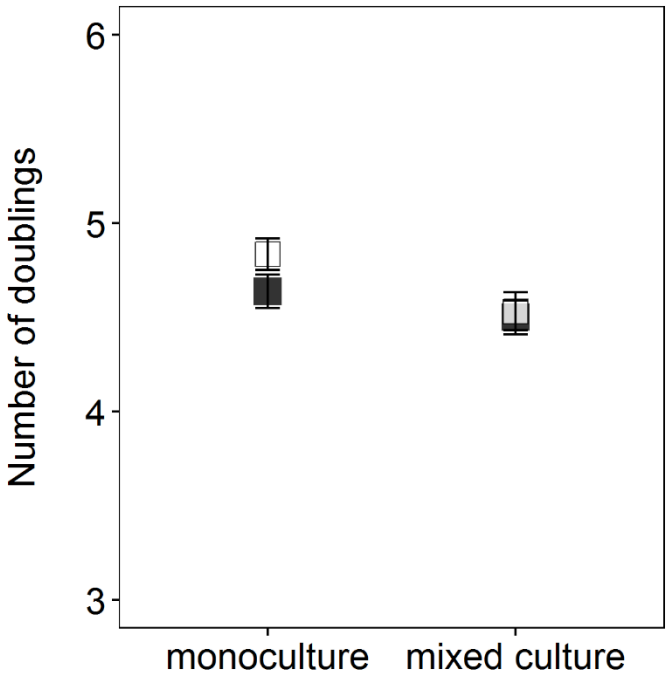

Figure S 2: There are no growth differences between the pyoverdine-producing strain (filled squares) and the non-producing strain (open squares) on agarose pads supplemented with 200 µM $FeCl_3$. Growth of the two strains was neither different in monoculture (t-test: t_{78} = -1.61, p = 0.11) nor in mixed culture (t-test: t_{71} = -0.23, p = 0.82). These results are in line with the view that pyoverdine production is completely stalled when iron is plentiful (Weigert et al. 2017), such that there is no more difference in the strains' phenotype. This also means that the fitness effects we observed in iron-depleted media (Figures 3 - 6) are attributable to pyoverdine-mediated social interactions. The number of doublings was calculated over a growth period of 3 hours. Symbols and error bars indicate means and standard errors of the mean, respectively.

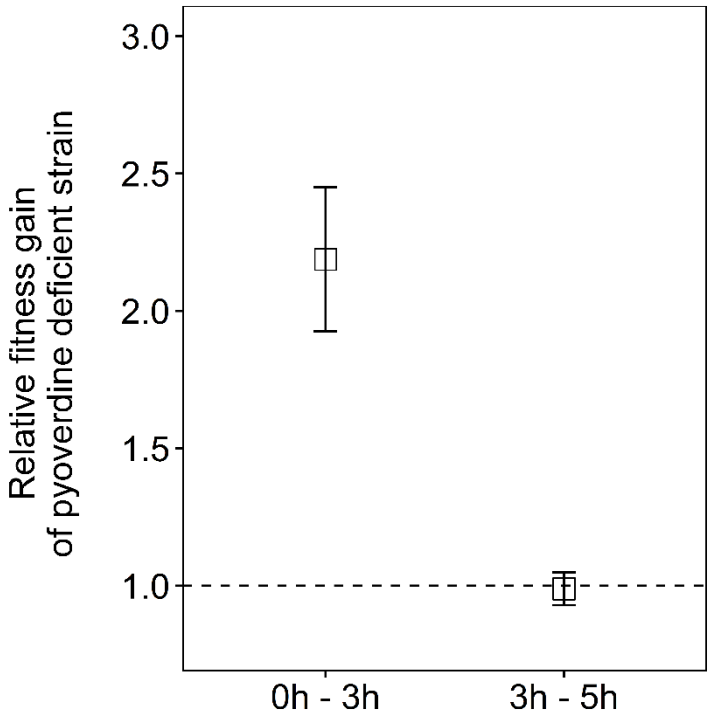

Figure S 3: Non-producers experience a significant relative fitness advantage during the first three hours of competition (zero to three hours; one sample t-test: $t_{20} = 4.53$, $p < 0.001$), but not during the later competition phase (three to five hours; one sample t-test: $t_{41} = -0.18$, $p = 0.85$). We used cell numbers to calculate strain frequencies at time point zero, three and five hours and to estimate the relative fitness of non-producers as $v = [q_2(1 - q_1]/[q_1(1 - q_2]$, where q_1 and q_2 are the initial and final frequencies of the non-producer (Ross-Gillespie et al. 2007). The dotted line represents the fitness equilibrium, where no strain has a relative fitness advantage over the other. Symbols and error bars indicate means and standard errors of the mean, respectively.